Building and Environment, Vol. 24, No. 4, pp. 325–333, 1989.
Printed in Great Britain.

0360–1323/89 $3.00 + 0.00

Computational Evaluation of Wind Effects on Buildings

A. BASKARAN*
T. STATHOPOULOS*

A computer simulation of wind flow around a block-shaped building has been attempted by using 3-D turbulent flow conditions. The Control Volume Method is used for numerical discretisation. The SIMPLE algorithm inter alia *fulfils the continuity condition. Results have been compared with previous computational attempts and also with data obtained in boundary layer wind tunnel tests. The inclusion of modifications in the standard* k–ε *model improves the prediction of pressures on the building envelope.*

NOMENCLATURE

a_P	hybrid difference scheme coefficient at node P
b	linearised source term
B	width of building
C_p	mean pressure coefficient
C_μ, C_1, C_2, C'_1, C'_1	turbulence model constants equal to 0.09, 1.44, 1.92, 2.24, 0.8
G	turbulence generation term
h	probe height from ground level
H	height of building
L	length of building
k	turbulent kinetic energy
K_1, K_2	constants equal to 0.27, −0.49
n	streamline co-ordinate
R_c	radius of curvature of streamline
s	streamline co-ordinate
S	source term of the difference equation
S_{ns}	shear strain
U_j	velocity vector
u_i, u_j	mean velocity components
u_g	velocity at gradient height
x, y, z	distance along the coordinate axis
z_g	gradient height

Greek symbols

α, β	constants equal to 1.5, 0.6
γ_{ij}	rate of production
Γ_ϕ	diffusion proportionality factor of ϕ
δ_{ij}	Kronecker delta ($=1$ if $i=j$; $=0$ if $i \neq j$)
ε	dissipation of turbulent kinetic energy
ν_t	turbulent viscosity
σ_κ, σ_ε	universal constants equal to 1.0, 1.3
ϕ	dependent variable, i.e. u, v, w, k, ε

INTRODUCTION

WIND VELOCITIES around buildings and wind-induced pressures on the building envelope have been considered as important design parameters. These are measured either in full-scale or in boundary layer wind-tunnels constructed to simulate the natural wind conditions in a laboratory environment. Results of such tests are utilised for the development of specifications required for wind standards and building codes of practice. However, problems of simulation and the increasing cost of wind tunnel testing are disadvantages in the experimentation.

Advancements of Computational Fluid Dynamics (CFD) and computer simulation techniques on the other hand, provide new approaches for the evaluation of wind effects on buildings. When comparing the speed and cost of computation, the latter appears to reduce by a factor of 10 every eight years (Fig. 1 [1]). For a 2-D problem requiring the solution of Navier–Stokes Equations (NSE), Table 1 indicates the significant decrease in computational time achieved with the progress in computer technology [2]. However, attempts to model the turbulent wind flow conditions around buildings have been made only recently.

Vasilic-Melling [3] first attempted the numerical modelling of wind both in 2-D and 3-D flows. Even though a good agreement with experimental data was found for 2-D flow over fences, the 3-D flow around surface mounted cubes was underpredicted, particularly at the downstream side of the obstacles. Hanson *et al.* [4] used the Random Vortex Method (RVM) of Chorin [5] and the Control Volume Method (CVM) of Caretto *et al.* [6] for wind flow simulation over a 2-D building model. Summers *et al.* [7] found that the RVM is not compatible with turbulence models and it also appears inefficient and expensive for the flow over 3-D sharp edge buildings. Using CVM, Hanson *et al.* [8] reported the 3-D simulation results without inclusion of any standard turbulence models. Comparisons between computed results and experimental data obtained in the wind tunnel were extensively made by Summers *et al.* [9]. It was concluded that the deficiency of the simulation—mainly its failure to represent the characteristics of the wake—could be improved by the inclusion of a detailed treatment on the turbulence.

Paterson [10] has attempted the solution of the 3-D Reynolds equations. The effect of turbulence in the flow has been accounted for by means of k–ε models. The discretisation of non-linear PDE's and the solution of linearised equations were obtained by following a pro-

*Centre for Building Studies, Concordia University, Montreal, Quebec, Canada H3G 1M8.

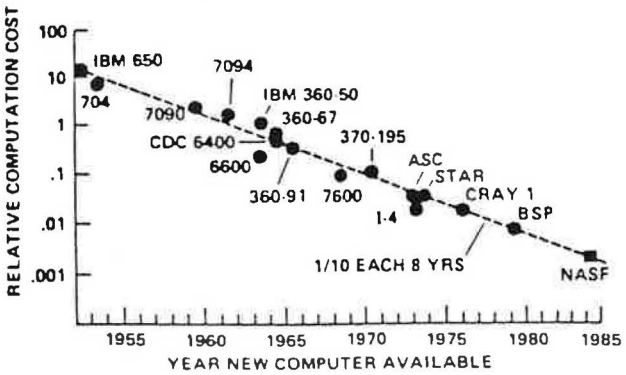

Fig. 1. Trend of relative computational cost for numerical flow simulation on large computers [1].

cedure similar to that of Vasilic-Melling [3]. Comparisons were made with wind tunnel experimental data as well as with full-scale measurements for an isolated building exposed to normal wind direction. Mathews [11] and Mathews and Meyer [12] made 2-D studies for the numerical modelling of wind loading on two different building geometries.

Recently, the unsteady wind conditions around buildings were studied by Murakami and Mochida [13] by means of supercomputers. The large eddy simulation technique is used to induce the necessary turbulence but computed parameters have not been compared with experimental data.

A general purpose computer program, named PHOENICS, has been developed by Spalding *et al.* [14] to provide the numerical solution for a variety of partial differential equations. Jansson [15] used this program to carry out 2-D and 3-D computations of wind flow around a square building of different heights. Computed pressure distributions on a flat roof were compared with measured wind tunnel data, as shown in Fig. 2. Although there is some general agreement between measured and computed pressure coefficients, the overestimation of computed suctions at the roof edge is clear. Differences between experimental and computed results may be partly due to different velocity inlet profile conditions. However, it appears that more emphasis should be given to the turbulence model and the appropriate boundary conditions used for the solution of such problems. Similar discrepancies have also been reported by Häggkvist *et al.* [16] who actually found only qualitative and non-quantitative agreement between results obtained through PHOENICS and experimental data.

This paper presents the necessary mathematical equations that can adequately describe the 3-D turbulent wind flow conditions around a building. Computations have been made by including the standard k–ε turbulence models of Launder and Spalding [17] and two modified versions as well. Comparisons with experimental data have been made and significant improvements, at least

Table 1. Comparison of computational times required for the solution of NSE in different computers [2]

Computer	CPU-time
UNIVAC 1106	100 days
ICL 2980	25 days
CDC CYBER 175	4 days
IBM 3081K	3 days
CDC 7600	2 days
CDC STAR 100	1 day
ICL DAP	13 h
HITACHI S9/1AP	10 h
FUJITSU 7890	10 h
ILLIAC IV	6 h
CRAY-1S	4 h
CYBER 205	4 h
CRAY-XMP	3 h

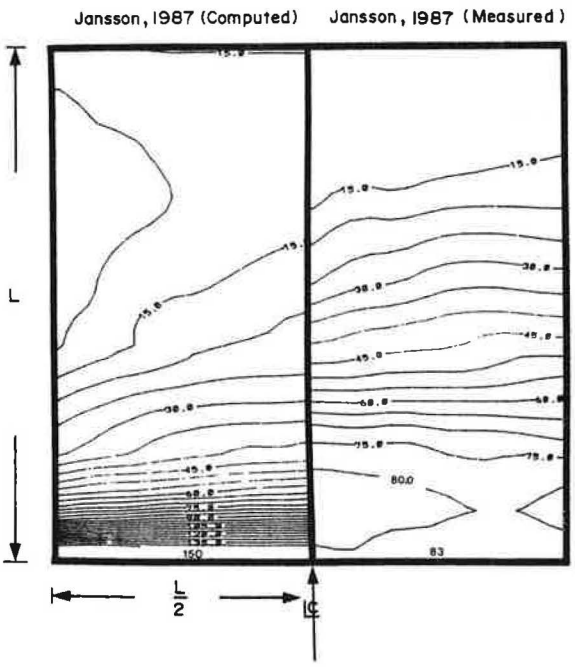

Fig. 2. Comparison of the computed mean pressure coefficients for a flat roof with the measured wind-tunnel values. The length to height ratio is 3 [15]. Note: pressure coefficients have been multiplied by −100.

for some cases, were identified when the modifications of the turbulence models are utilised.

COMPUTATIONAL METHODOLOGY

In developing the finite difference version for the Navier–Stokes equations it is more convenient to deal with a single general equation for any dependent variable. A compact form for the necessary differential equations can be expressed in cartesian tensor notation as:

$$U_j \frac{\partial \phi}{\partial x_j} = \frac{\partial}{\partial x_j}\left[\Gamma_\phi \frac{\partial \phi}{\partial x_j}\right] + S. \tag{1}$$

In this equation U_j denotes the velocity vector. The left hand side represents the transport by convection of any dependent variable ϕ. On the other hand, the first term on the right hand side of equation (1) represents the diffusion of ϕ with proportionality factor Γ_ϕ. The second term represents the source S, which is related to the generation or destruction of ϕ, denoted by S_c, as well as any other quantity (S_p) not accounted for in the convection and diffusion expression, i.e.

$$S = S_c + S_p. \tag{2}$$

Details of the individual terms of equations (1) and (2) when the dependent variable ϕ represents the velocity components u, v and w, the turbulent kinetic energy k and its dissipation ε are provided in Table 2.

Note that $\partial p/\partial x_i$ is the pressure gradient, G is the generation term and ν_t is the fluid turbulent viscosity calculated by:

$$\nu_t = C_\mu \frac{k^2}{\varepsilon}, \tag{8}$$

in which C_μ, σ_κ, σ_ε, C_1 and C_2 are universal constants getting the values 0.09, 1.0, 1.3, 1.44 and 1.92 respectively. In addition to equations (3)–(7), continuity has also been included to fulfil the law of conservation of mass.

Difference equations can be formulated for the differential equations by using the control volume method. Details of the general discretization procedure are well documented in the literature, e.g. Patankar [18]. Discretization details for the particular equations representing wind flow conditions can be found elsewhere (see Vasilic-Melling [3] and Paterson [10]). The final algebraic equations take the form:

$$a_P \phi_P = \left(\sum_{i=1}^{n} a_i \phi_i\right) + b, \tag{9}$$

in which: P is the grid node on which the dependent variable ϕ is computed; n is the number of nodes surrounding P; a_i is the hybrid difference scheme coefficient; b is the linearised source term.

A similar equation can be derived for the pressure term of the momentum equation. The well-known SIMPLE algorithm, Patankar [18], is used to correct the velocities and to improve the initially assumed pressure field. The advantageous staggered grid arrangement is used. Specification of pressure values on boundaries is not required by placing the boundaries of the computational domain and the boundaries of the building envelope on the velocity nodes of the staggered grid. The following boundary conditions are used in the computation.

Inlet: a power law profile $[u/u_g = (z/z_g)^\alpha]$ for the x-component velocity u, whereas the other two velocity components v and w are computed from potential flow equations. The initial turbulence properties (k and ε) are computed by using the semi-empirical formula of Launder and Spalding [17] based on the calculated velocity field. *Outlet, Top and Side*: Dirichlet boundary conditions are applied by using the initially calculated values. *Ground and Building Envelope*: perpendicular velocity components are assumed to be zero, whereas tangential velocities and turbulence properties are calculated by using the universal wall functions of Launder and Spalding [17].

COMPUTED RESULTS AND MEASURED DATA

In this section the computed values obtained by using the standard k–ε turbulence models are compared with the measured wind tunnel values and also with the results of previous computational attempts. Computations are made by using the VAX 11/785 computer. Comparison data include wind-velocities around the building and wind generated pressures on the building envelope.

Figure 3 shows one such comparison for the time-averaged $\bar{u}$ velocity component. Data are presented as percentages of velocity ratios referenced to free stream values for a particular location. Results are compared for a number of points on two locations upstream of the building for flow normal to the building face. Due to symmetry, both measurements and computations were made only for half of the flow domain at two heights of approximately 5 and 16 cm representing 10 and 31 m respectively in full scale. Three curves on each set represent the computed values of the present study; the

Table 2. Terms of equations (1) and (2)

ϕ	Γ_ϕ	S_c	S_p	Equation
u, v, w	ν_t	$-\frac{\partial p}{\partial x_i}$	0	(3), (4), (5)
k	$\frac{\nu_t}{\sigma_\kappa}$	G	$-\varepsilon$	(6)
ε	$\frac{\nu_t}{\sigma_\varepsilon}$	$C_1 G \frac{\varepsilon}{k}$	$-C_2 \frac{\varepsilon^2}{k}$	(7)

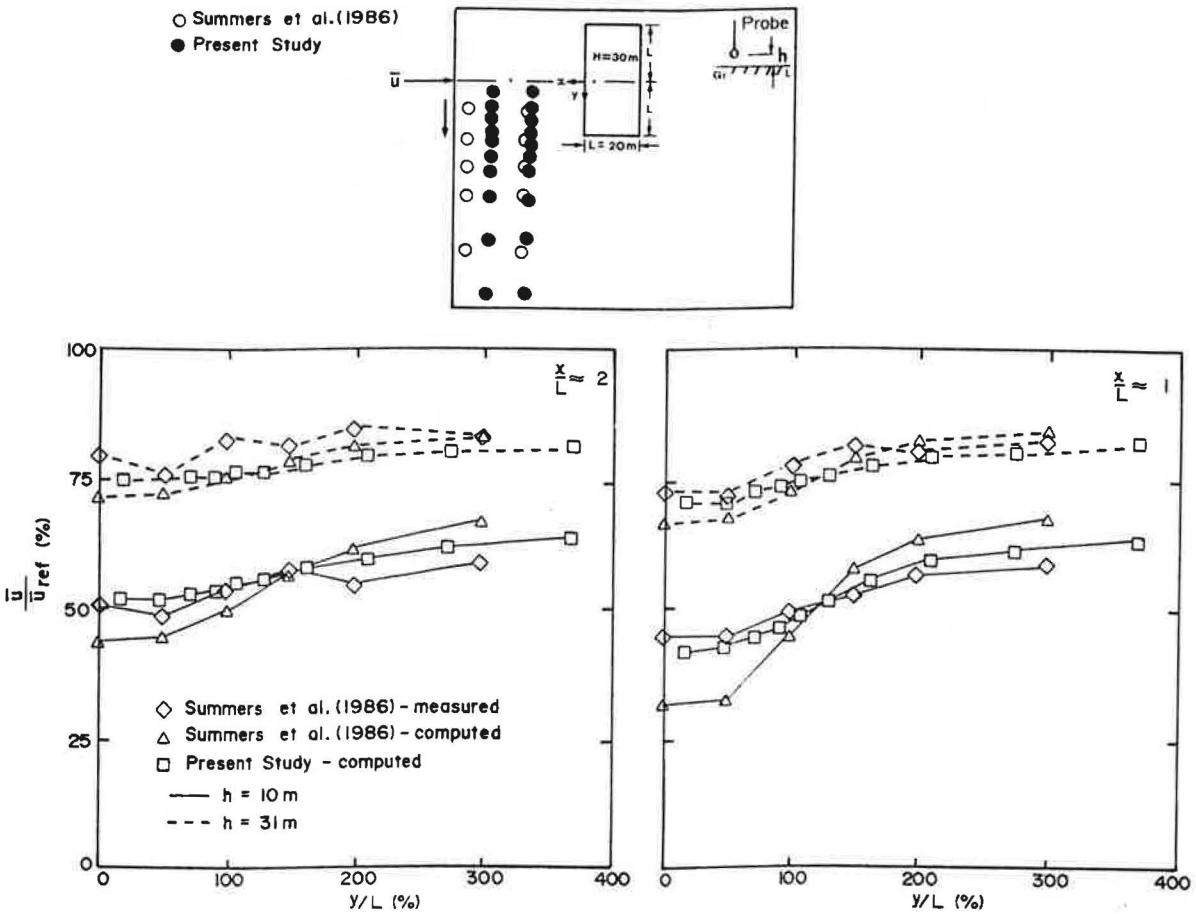

Fig. 3. Comparison of the upstream wind velocities with and without inclusion of turbulence models.

computed values of Summers *et al.* [9]: and the wind tunnel data also reported by them.

From the comparison it is clear that the computational tools can predict the overall nature of the flow conditions. However, deviations from the wind tunnel values smaller than those of Summers *et al.* [9] are noted for the computed data of the present study. A similar feature appears in Fig. 4, which shows comparisons for two downstream locations, in the same format as in Fig. 3. Poor agreement of both sets of computational values is evident near the building. However, the values obtained in the present study are generally closer to the wind tunnel data. Note that the solution grids are slightly different and did not exactly correspond in the two studies but this makes little difference in these comparisons. The pertinent question of Summers *et al.* [9]: "*Whether the most obvious deficiency of the simulation—its failure to reproduce the compactness of the wake—could be improved by the introduction of a more detailed treatment of turbulence*," is considered in the present study, in which the turbulent nature of flow is incorporated in the computation by using the well-known k–ε models. The better agreement of present results with the experimental data is attributed to this additional mathematical treatment of the flow.

Figure 5 compares the measured with the computed velocity fields around a tall building. The measured values are taken from experiments carried out in a boundary layer wind tunnel by Stathopoulos [19]. Velocity amplification factors $(u_{10})P/(u_{10})A$, i.e. mean wind speed in the presence of the building divided by the mean wind speed in the absence of the building, at 10 m above the ground level, are presented in contour form. Since both velocities are measured at the same height, these ratios directly provide the changes in flow conditions due to the presence of the building. Ratio values less than unity indicate a reduction of wind speed in the presence of the building. On the other hand, high velocity amplification ratios are measured as well as computed near the building corners. Although the overall trends in both measured and computed values are similar, some differences may be explained by the much denser grid used in the computation.

Comparisons between computed and measured pressures on the building envelope have also been made to establish the adequacy of the computational approach. Pressures are converted into the conventional form of non-dimensional pressure coefficients normalized with the dynamic pressure at the building roof height.

Jansson [15] reported such pressure coefficients measured at various tap locations on the flat roof of a building model placed in a wind tunnel. To exclude the errors induced due to differences between the grid nodes of computation and measurement locations, computational grids were placed exactly at the measurement locations.

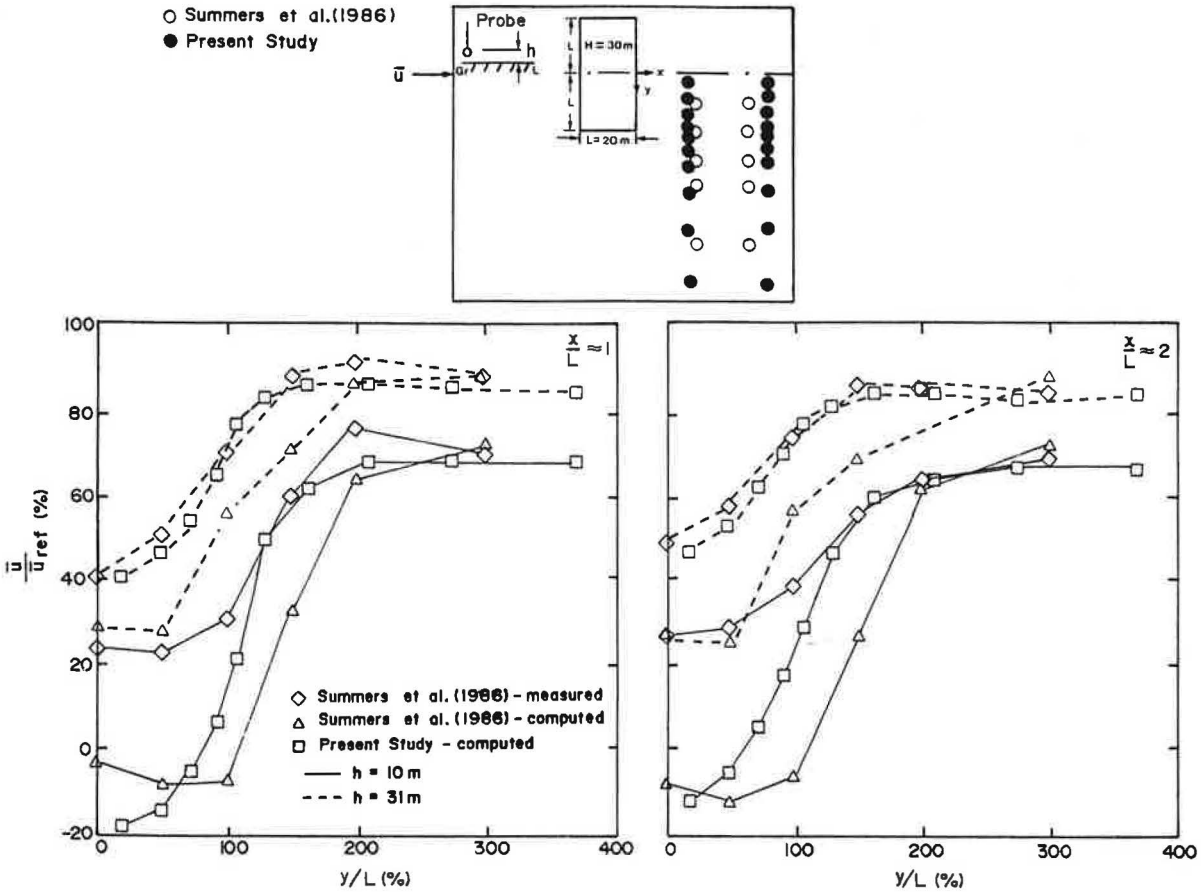

Fig. 4. Comparison of the downstream wind velocities with and without inclusion of turbulence models.

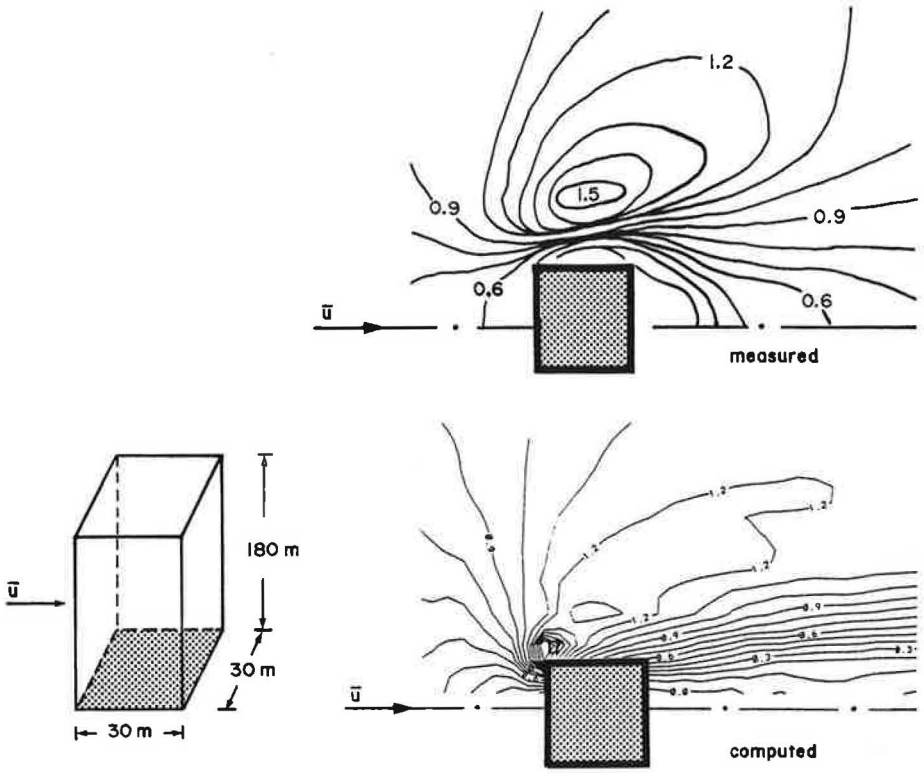

Fig. 5. Comparison of the windspeed amplification factors measured around a tall building and computed by using the standard k–ε turbulence model.

Figure 6 shows the results of this comparison. Values computed along the centre line of the roof by using the PHOENICS program (Jansson, [15]) form a steeper gradient from the leading edge in comparison to that of the measured data. On the other hand, computed data of the present study are closer to the measured values on the windward half of the roof, but this agreement breaks down near reattachment. Thus it appears that the mathematical equations based on the k–ε turbulence model are inadequate for the modelling of the turbulence generated by smaller eddies near the reattachment zone.

In Figure 7 pressure coefficients are plotted against the ratios of Z/H, where Z is the height of the pressure tap or the grid location measured from the ground level and H is the building height. The variation of positive values of pressure coefficients on the windward wall and negative values on the leeward and side walls is shown along the centre line of each wall surface. The measured data have been received from boundary layer wind tunnel tests described in Zhu [20]. The agreement between measured and computed values is encouraging for the windward wall. The pressure coefficient is maximum at about 2/3 of the windward height (stagnation point). However, in the case of side and leeward walls, the induced suctions are significantly underestimated by the computational procedure.

Thus, it is clear that the separated flows demand better mathematical treatment in the computation and this is the subject of the next section.

MODIFICATION TO THE k–ε TURBULENCE MODELS

As previously mentioned, the fluid turbulent viscosity has been calculated by equation (8), in which the proportionality factor C_μ is equal to 0.09. Based on experimental observations, Rodi [21] reported that C_μ will vary from 0.03 to 0.7 depending on the flow region. An algebraic relation has been derived for the Reynolds stress with a correction that can account for the variation of C_μ. This is known as streamline curvature correction, Gibson [22]. The algebraic equation balancing the rate of production (γ_{ij}) of the Reynolds stress ($\overline{u_i u_j}$), pressure-strain and dissipation can be written, Leschziner and Rodi [23], as:

$$\frac{\overline{u_i u_j}}{k} = \frac{1-\beta}{\alpha\varepsilon}\gamma_{ij} - 2/3\frac{\delta_{ij}}{\alpha}(1-\alpha-\beta), \tag{10}$$

in which δ_{ij} is the well-known Kronecker delta. For local equilibrium of turbulence energy, expressed by $\gamma_k = \varepsilon$, the constants α and β are equal to 1.5 and 0.6 respectively. Converting (i,j) into streamline coordinates (s,n) the fluid turbulent viscosity can be redefined as:

$$\nu_t = \left\{\frac{-K_1K_2}{1+0.57\frac{k^2}{\varepsilon^2}\left(\frac{\partial u_s}{\partial n}+\frac{U_s}{R_c}\right)\frac{U_s}{R_c}}\right\}\frac{k^2}{\varepsilon}, \tag{11}$$

where the bracket represents the proper expression for

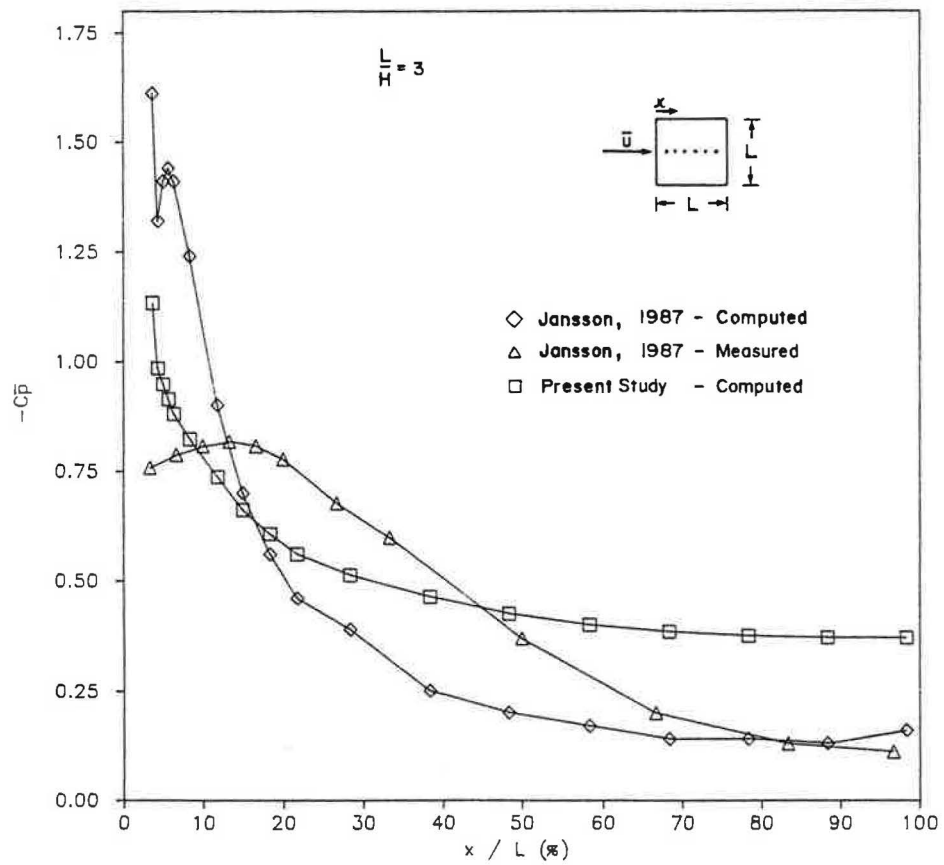

Fig. 6. Mean pressure coefficients on a flat roof.

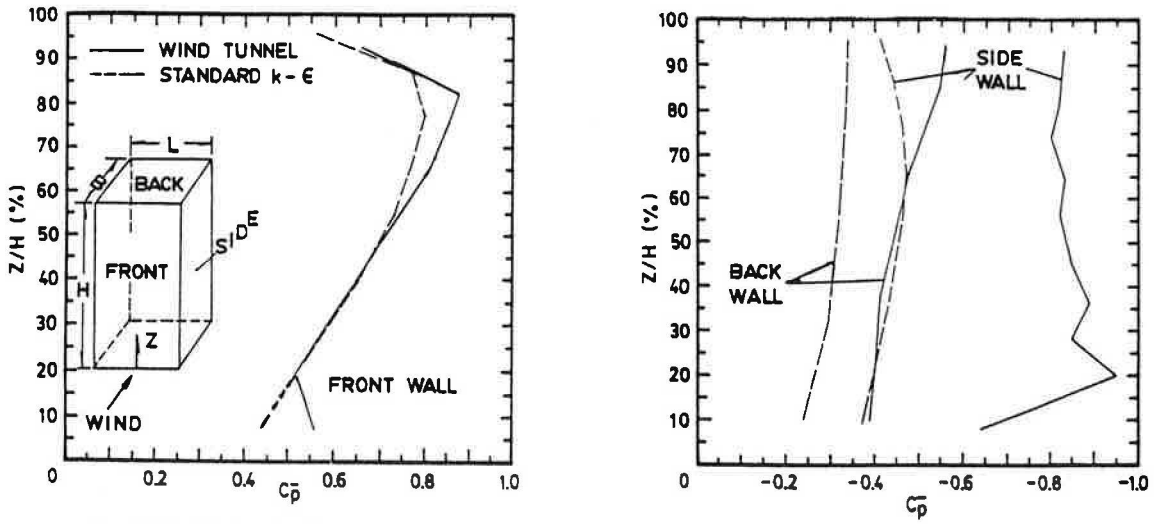

Fig. 7. Wind-induced wall pressures on a tall building computed by using the standard k–ε turbulence model.

C_μ. Note that u_s is the velocity along the streamline s with radius of curvature equal to R_c; U_s is the sum of the velocities u and v; and K_1, K_2 are constants equal to 0.27 and -0.49 respectively. The expression for C_μ is evaluated for each grid node during the computation. However, the negative velocities at the recirculation zone produce a negative C_μ which is not feasible. To overcome this difficulty, C_μ is not allowed to take a value less than 0.09 (the same as in the case of the standard k–ε model). Similarly, a value of 0.09 for $-K_1K_2$ was used in the computation instead of the actual value which is 0.13 (Durao *et al.* [24]). Therefore, the equation used in the present study takes the form:

$$C_\mu = \max\left\{0.09, \frac{0.09}{1+0.57\dfrac{k^2}{\varepsilon^2}\left(\dfrac{\partial u_s}{\partial n}+\dfrac{U_s}{R_c}\right)\dfrac{U_s}{R_c}}\right\}. \quad (12)$$

In addition to the streamline curvature correction, a modification on the dissipation of k, originally proposed by Hanjalic and Launder [25], has also been implemented. In equation (7), the second term of RHS can be viewed as production of ε defined as:

$$\gamma_\varepsilon = C_1 G\frac{\varepsilon}{k}, \quad (13)$$

where the value $C_1 = 1.44$ is used in the standard k–ε model. An increase in C_1 leads to a direct increase in ε and indirectly it causes reduction in the turbulence level, k. Due to this combined effect, the turbulent viscosity [equation (11)] will be reduced, i.e. the flow will become less viscous. In order to enhance the diffusion process by promoting the formulation of smaller eddies, on which the normal stresses are more effective than the shear stresses, Leschziner and Rodi [23] suggested the use of:

$$\gamma_\varepsilon = [C_1' G - C_1'' \gamma_t S_{ns}^2]\frac{\varepsilon}{k}, \quad (14)$$

where S_{ns} is the shear strain in the direction of streamline; and C_1' (=2.24) and $C_1''(=C_1'-C_1)$ are modified constants to be used instead of C_1.

The streamline curvature correction [equation (12)] and the preferential dissipation correction [equation (14)] have both been utilised in the present study in an attempt to better represent the separated flow characteristics. Computations were repeated by keeping the other parameters of the program constant. The new results were then compared with those obtained by using the standard k–ε model. Figure 8 displays the side view of the streamline plots for a tall building exposed to normal wind. The building is 120 m high and has a square cross-section of 60×60 m. The streamlines are depicted for the plane passing through the centre of the building and are obtained based on the combination of the velocity vectors u and w to identify the flow path. The x-coordinate is normalised by the length of the building ($L = 60$ m). The building height ($H = 120$ m) is used to normalise the vertical z-coordinate. Clearly the length of the recirculation zone increases when the modifications of the k–ε model are utilised. The prediction of pressures on the building envelope also improves.

Figure 9 presents the newly computed pressure coefficients along with the old values and the measured data in the same format as in Fig. 7. The modifications implemented in the k–ε model reduce the differences between experimental data and computed values for all the walls. Although pressure coefficients are marginally affected on the windward wall, there is significant improvement in suctions computed on the side wall. This can be related to the improved representation of recirculation zones and involved eddies, as previously shown in Fig. 8. Improvements in the separation of the flow on the side of the building, and the modified curvature of the shear-layer also increase suctions on the back wall. The suggested modifications provide better agreement with the wind-tunnel pressure coefficients, but further improvement is still required.

The inclusion of two additional equations [equations (12) and (14)] in the computer coding naturally demands

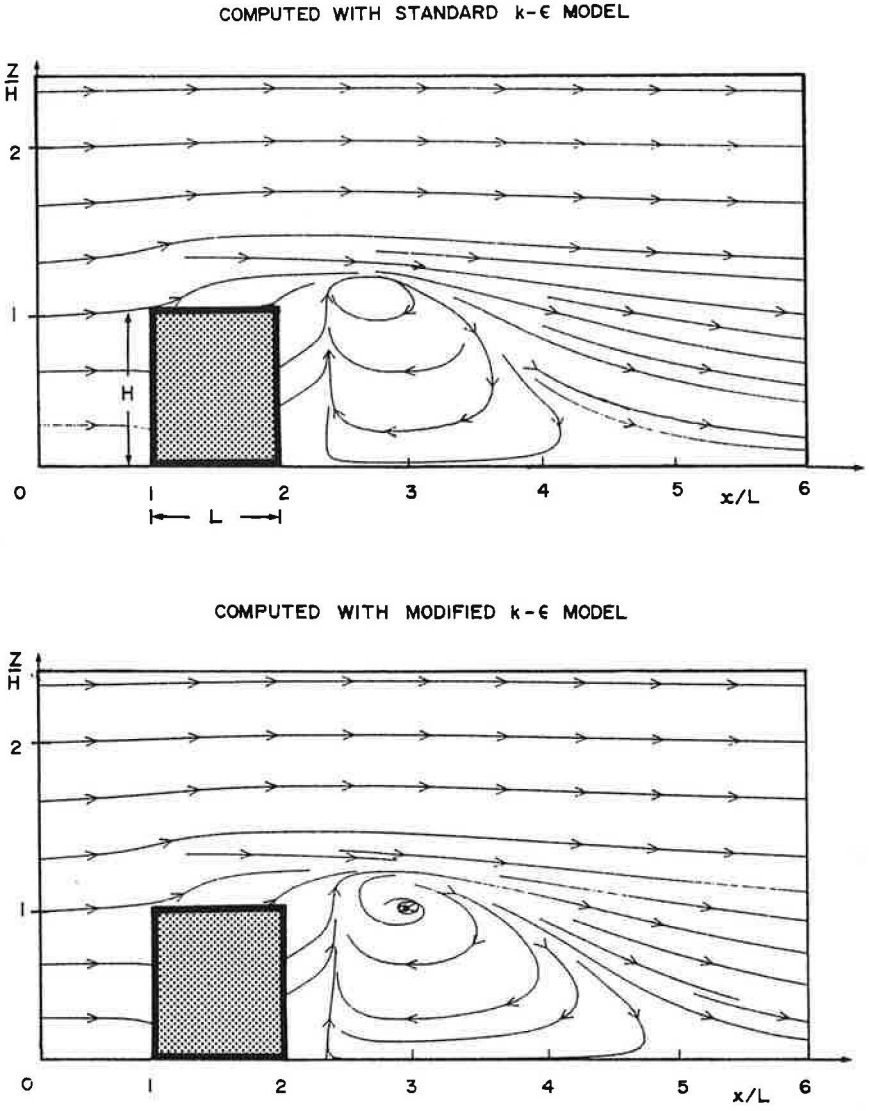

Fig. 8. Streamline plots for the recirculation zones in the wake of a tall building by using the standard and the modified k–ε model.

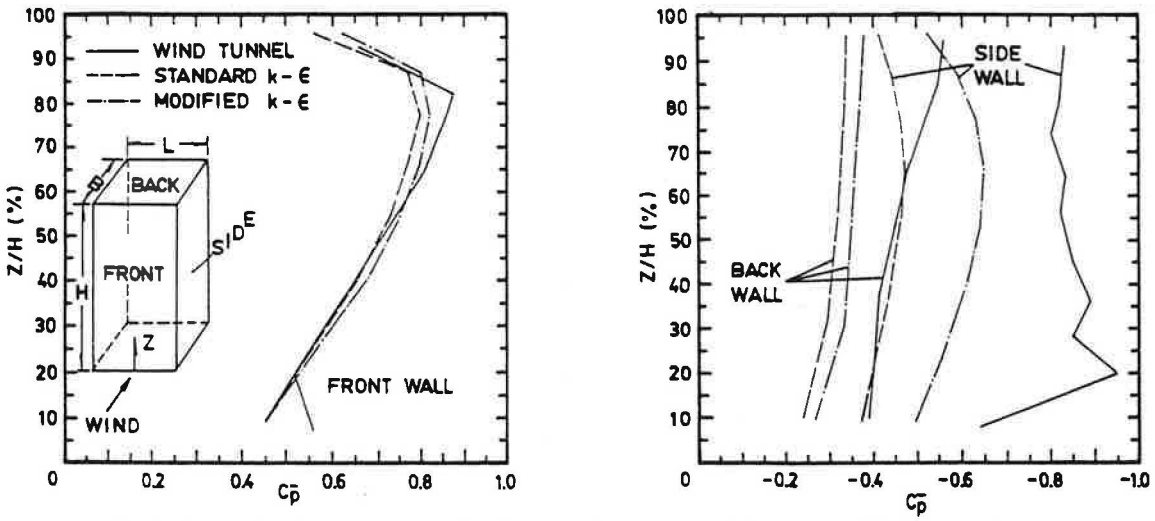

Fig. 9. Comparison between computed and measured pressure coefficients on a tall building envelope.

more computer resources. Nevertheless, the improvements in the predicted pressures would justify these additional resources.

CONCLUSIONS

The following conclusions can be made from the results presented in this paper regarding the computational evaluation of wind effects on a block-shaped building.

(1) The inclusion of turbulence in the wind flow around buildings by using the standard k–ε turbulence model in the computational procedure improves the predicted velocity fields.

(2) The semi-empirical k–ε turbulence model along with its "universal constants" underestimate the size of the recirculation zones and involved eddies.

(3) Two simple modifications made to the k–ε turbulence model reduce the difference between measured and computed pressures on the building envelope.

REFERENCES

1. D. R. Chapman, Computational aerodynamics development and outlook. *J.AIAA* **17**, 1293–1313 (1979).
2. W. Glentzsch. Vectorization of computer programs applied to computational fluid dynamics. *Notes on Numerical Mechanics*, Vol. 8. Viewg and Sohn, Brawschweigh (1987).
3. D. Vasilic-Melling, Three-dimensional turbulent flow past rectangular bluff-bodies. Ph.D. Thesis, University of London (1977).
4. T. Hanson, D. M. Summers and C. B. Wilson, Numerical modelling of wind flow over buildings in two dimensions. *Int. J. Numerical Meth. Fluids* **4**, 25–41 (1984).
5. A. J. Chorin. *A Mathematical Introduction to Fluid Mechanics*. Springer-Verlag, New York (1979).
6. L. S. Caretto. R. M. Curry and D. B. Spalding, Two numerical methods for three-dimensional boundary layers. *Comput. Methods appl. mech. Engng* **1**, 39–57 (1972).
7. D. M. Summers, T. Hanson and C. B. Wilson, A random vortex simulation of wind flow over a building. *Int. J. Numerical Meth. Fluids* **5**, 849–871 (1985).
8. T. Hanson, D. M. Summers and C. B. Wilson, A three-dimensional simulation of wind flow around buildings. *Int. J. Numerical Meth. Fluids* **6**, 113–127 (1986).
9. D. M. Summers, T. Hanson and C. B. Wilson, Validation of a computer simulation of wind flow over a building model. *Bldg Envir.* **21**, 97–111 (1986).
10. D. A. Paterson, Computation of wind flow over three-dimensional buildings. Ph.D. Thesis, University of Queensland, St. Lucia, Queensland, Australia (1986).
11. E. H. Mathews, Prediction of the wind generated pressure distribution on buildings. *J. Wind Engng Ind. Aerodyn.* **25**, 219–221 (1987).
12. E. H. Mathews and J. P. Meyer, Numerical modelling of wind loading on a film clad greenhouse. *Bldg Envir.* **22**, 129–134 (1987).
13. S. Murakami and A. Mochida, Three-dimensional numerical simulation of air flow around a cubic model by large eddy simulation. *J. Wind Engng. Ind. Aerodyn.* **25**, 291–305 (1987).
14. D. B. Spalding, A general purpose computer program for multi-dimensional one and two phase flow. *Math. Comput. Simulation* **8**, 267–276 (1981).
15. O. B. Jansson, Tryckberäkning kring smäklossar, Ser. Anr. 149. Water Resources Engineering, Luleä, Sweden (1987).
16. K. Häggkvist, C. Anderson and R. Taesler, PHOENICS—Applications in building climatology, *Numerical Simulation of Fluid Flow and Heat/Mass Transfer Processes*, Lecture Notes in Engineering, Vol. 18. Springer, Berlin (1986).
17. B. E. Launder and D. B. Spalding, The numerical computation of turbulent flows. *Comput. Methods appl mech. Engng* **3**, 269–289 (1974).
18. S. V. Patankar, *Numerical Heat Transfer and Fluid Flow*. McGraw-Hill, New York (1980).
19. T. Stathopoulos, Wind environmental conditions around tall buildings with chamfered corners. *J. Wind Engng Ind. Aerodyn.* **21**, 71–87 (1985).
20. X. Zhu, Wind pressures on buildings with appurtenances, M.Eng. (Building) thesis, Concordia University, Montreal (1987).
21. W. Rodi, A note on the empirical constant in the Kolmogorov–Prandtl eddy-viscosity expression. *J. Fluids Engng Trans. ASME*, 386–389 (1975).
22. M. M. Gibson, An algebraic stress and heat-flux model for turbulent shear flow with streamline curvature. *Int. J. Heat Mass Transfer* **21**, 1609–1617 (1978).
23. M. A. Leschziner and W. Rodi, Calculation of annular and twin parallel jets using various discretization schemes and turbulence model variations. *J. Fluids Engng Trans. ASME* **103**, 352–360 (1981).
24. D. F. G. Durao, M. V. Heitor and J. C. F. Pereira, The turbulent flow in the near-wake of a squared obstacle. Proceedings of 1987 ASME Applied Mechanics, Bio-Engineering and Fluids Engineering Conference, Cincinnati OH, pp. 45-50 (1987).
25. K. Hanjalic and B. E. Launder, Preferential spectral transport by irrotational straining. *Turbulent Boundary Layers, ASME*, 101–110 (1979).